

Minimization of Nyquist ghosting for fMRI at ultra-high fields based on a ‘negative read-out gradient’ strategy.

W. van der Zwaag^{1,2}, H. Lei^{1,2}, N. Just^{1,2}, J. Marques^{1,2}, and R. Gruetter^{1,3}

¹Laboratory for functional and metabolic imaging, Ecole Polytechnique Federale de Lausanne, Lausanne, Switzerland, ²Department of Radiology, University of Lausanne, Lausanne, Switzerland, ³Departments of Radiology, Universities of Lausanne and Geneva, Switzerland

Introduction

Nyquist ghost correction approach in echo planar images typically is based on a reference scan acquired in the absence of the blipped phase encode gradient. However, although a substantial ghost reduction is achieved, residual artefacts remain. It has been reported that further artefact reduction is possible using a ‘negative gradient read-out’ strategy where the phase encoded image is acquired with reversed polarity of the read-out gradient (G_x) in a reference scan [1]. The aim of the present study was to extend this approach to acquiring time-series of fMRI measurements by alternating the read-out polarity, i.e. the ‘positive’, G_x , and ‘negative’, $-G_x$, echo trains and to evaluate three resulting strategies for ghost removal.

Theory

The k-space signal for EPI can be written as:

$$S(k_x, k_y) = \iint m(x, y) \exp \left(2\pi i \left[\Delta f(x, y) \left(T_n + (-1)^n \left(\frac{k_x}{\gamma G_x} \right) \right) + k_x x + k_y y \right] \right) dx dy$$

where $m(x, y)$ represents the object’s transverse magnetisation, $\Delta f(x, y)$

the frequency distribution, and T_n is the time at the centre of the nth k-space line. Because Δf depends on x and y and increases with B_0 , the inconsistencies between odd and even k-space lines, responsible for Nyquist ghosting, depend on k_y as well as k_x [1] and increase with magnetic field. Inverting the polarity of G_x , which amounts to a replacement of $(-1)^n$ with $(-1)^{n+1}$ in Eq. 1, was used for Nyquist ghost correction in fMRI time series using the following three strategies: The first, denoted (P): After Fourier transformation in the read direction, (fft_x) , the phase difference between the ‘positive’ and ‘negative’ image is used to correct both. 2 (A): After fft_x , the ‘positive’ and ‘negative’ images are summed and then fft_y is applied to create a new image. 3 (CP): The phase of the result of (A), before FTT along the phase-encode direction (fft_y), is combined with the amplitude of the ‘positive’ or ‘negative’ data to form ‘Corrected Phase’ data. In all three schemes, after phase correction, fft_y is applied to obtain images. Scheme CP and P allow a Nyquist ghost correction while preserving the temporal resolution, provided the BOLD response does not change the phase of the voxel appreciably. This change is likely minimal, as $TE \gg T_{2^* \text{ venous}}$ at 9.4T [2].

Methods

All experiments were performed in an actively shielded 9.4 T/31-cm with 12-cm gradient (400 mT/m in 120 μ s) using a quadrature ¹H RF-coil. The standard EPI sequence was modified to alternate the read-out direction every other volume. 300 volumes were acquired with $TE=25$ ms, $TR=2$ s. The first two volumes in each train were reference scans acquired without phase-encode blips. Following 2nd-order shimming with FASTMAP, 10 slices with a matrix size of 64 * 64, FOV of 25 * 25 mm and slice thickness 1 mm were acquired per volume. All images were corrected using the scans acquired without phase encoding, providing the ‘comparison image’. Further correction was done using methods P, A and CP.

Four male SD rats underwent an fMRI study employing a forepaw stimulation task. The employed block paradigm consisted of a 30s ON-period followed by 60s OFF, repeated 6 times. The animals were continuously monitored and maintained under good physiological conditions.

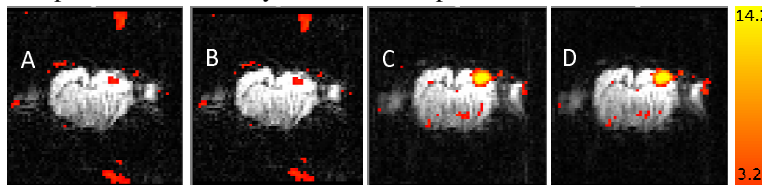


Figure 2 Single slices taken from Z-score maps shown overlaid on EPI images from the fMRI train. A: Comparison image. B: correction (P) C: Correction (CP) D: Correction (A)

Results and Discussion

EPI images of a rat brain phantom showed persistent ghosting in the comparison image (Fig 1A). Applying the three schemes resulted in similar ghosting levels of 2.5% (a 61% reduction) using schemes P and CP, while the result of scheme A was virtually ghost free (Fig.1), though this comes at the expense of a two-fold reduction in temporal resolution. In the fMRI data, ghosting intensity after correction was decreased by $41 \pm 30\%$ for P, by $67 \pm 10\%$ for CP and by $70 \pm 8\%$ for A (mean \pm sd). When false positive activation in the ghost region was detected, it was removed using scheme CP and A (Fig.2). The average number of voxels determined ‘active’ in the somatosensory cortex increased significantly using scheme CP and A: by $40 \pm 17\%$ and $25 \pm 14\%$ compared to the comparison data, respectively. Using scheme P a small non-significant increase was found. Average maximum Z-scores found were: $14.0 \pm 0.7\%$ in the comparison data and $13.9 \pm 0.6\%$, $15.5 \pm 2.9\%$ and $14.7 \pm 2.7\%$ using schemes P, CP and A, respectively.

In conclusion: substantial Nyquist ghost reduction is possible. While scheme CP has the advantage of preserving the temporal resolution, scheme A is readily suitable for applications requiring signal averaging, such as perfusion and/or diffusion experiments.

References 1. Hu. et al. Magn Reson Med. 1996; 36:166-71. 2. Lee et. al. Magn Reson Med. 1999; 42:919-928

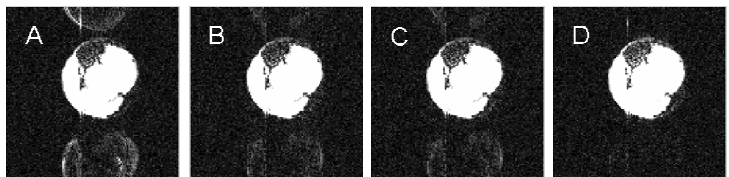


Figure 1 A: Comparison image. B: correction (P) C: Correction (CP) D: Correction (A). All images have been scaled to obtain identical image brightness in the noise.

fMRI analysis was carried out using FEAT in FSL. fMRI data were realigned and spatially and temporally smoothed. A GLM was formed with the BOLD signal change modelled as a box-car function convolved with the canonical HRF. Z-score maps were thresholded using clusters determined by $Z > 3.2$ and $P_{\text{corr}} = 0.05$. Remaining ghost levels and number of active voxels in the somatosensory cortex were measured.